Journal of Engineering and Development

www.jead.org
Vol. 20, No.02, March 2016
ISSN 1813-7822

EXPERIMENTAL STUDY OF HEAT TRANSFER OF AXISYMMETRIC AIR IMPINGEMENT FROM AN ORIFICE ON A MODIFIED SURFACE

*Dr. Adnan A. Abdul Rasool[1], Hadel Abdulhadi Jassim[2]

1) Assist Prof., Department of Mechanical Eng., Al-Mustansiriaya University, Baghdad Iraq.
2) M.Sc. Student, Department of Mechanical Eng., Al-Mustansiriaya University, Baghdad, Iraq.

(Received: 21/1/2015; Accepted: 27/5/2015)

Abstract: Impingement cooling jet is widely used in different industrial applications due to high rate of heat removal on the surface being subjected to impinging. Ribs are used to enhance convective heat transfer by the promotion of higher turbulence levels. The aim of present work is to perform an experimental verification of the using modified surface with ribs on heat transfer enhancement. Experiments were performed to characterize heat transfer to a normally impinging air jet on uniformly heated surfaces modified with ribs from a single orifice of different diameters D of (5, 12, 20 mm). A centrifugal blower is used for air impinging with jet velocity in the range (18.4-36 m/s). Local heat transfer distribution on the impingement surface is investigated for orifice-to-plate spacing ratio (Z/D) of (4, 6, 8, 10) using thermal infrared imaging technique. Different configurations of modified surfaces in form of ribs surface are studied in the present work which are: rectangular ribs, and circular ribs with different sizes spaced at different pitch on the target ribbed surface. Heat transfer enhancement for five rib geometries is evaluated by comparison with results for a smooth flat surface. The enhancement ratio of heat transfer, as compared to the smooth flat surface is demonstrated by a factor ranging from 1.2 to 3. It is observed that the different shape of the ribs cause different effects on heat transfer coefficient between the impinging air jet and the target plate. Also it is found that the orifice diameter, orifice to plate spacing ratio and jet velocity are the most effective variable which characterizes the heat removal rate.

Keywords: *Impingement jet cooling, Rib roughened wall, Heat transfer enhancement.*

دراسة عملية لانتقال الحرارة من اصطدام الهواء المتماثل من الفوهة الدائرية على الصفيحة المعدلة

الخلاصة: يستخدم التبريد التصادمي على نطاق واسع في التطبيقات الصناعية المختلفة نظرا لارتفاع معدل إزالة الحرارة على السطح المعرض للاصطدام . وتستخدم الأضلاع (Ribs) لتعزيزالحمل حراري عن طريق زيادة الاضطراب بمستوى أعلى. والهدف من العمل الحالي هو إجراء التحقق التجريبي من استخدام السطوح المعدلة مع الأضلاع على تعزيز نقل الحرارة. وأجريت التجارب لتوصيف نقل الحرارة إلى الهواء بواسطة نفث الهواء العمودي على الأسطح الساخنة المستوية والمعدلة بالأضلاع من فوهة دائرية ذات قطر (5، 12، 20 مم). يتم استخدام منفاخ الطرد المركزي لبثق الهواء مع سرعة في نطاق (18،4 - 36 م / ث). تم التحقيق في توزيع نقل الحرارة المحلي على سطح اصطدام البثق ونسبة بعد الصفيحة الهدف عن الفوهة الى القطر (10,8,6,4) باستخدام تقنية التصوير الحراري بالأشعة تحت الحمراء. تم دراسة اشكال مختلفة من السطوح المعدلة بالاضلاع في هذا العمل وهي: الأضلاع مستطيلة الشكل والاضلاع الدائرية ذات أحجام مختلفة بابعاد مختلفة على سطح الهدف. تم تقييم تحسين نقل الجرارة من خلال المقارنة مع النتائج لسطح مستو. نسبة تحسين نقل الحرارة، بالمقارنة مع سطح أملس يتجلى بمعامل يتراوح بين 1.2 إلى 3. ويلاحظ ان الشكل المختلف من الاضلاع يسبب

*Corresponding Author alaaazawy@yahoo.com

تاثيرات مختلفة على معامل انتقال الحرارة بين اصطدام الهواء ولوحة الهدف. ايضا وجد ان قطر الفتحة ونسبة بعد الصفيحة الهدف عن الفوهة الى القطر وسرعة الهواء هي المتغيرات الأكثر فعالية التي تميز معدل إزالة الحرارة.

1. **Introduction**

Impingement cooling heat transfer has been studied extensively in the past due to its wide application in cooling the walls of high temperature thermal systems. The air-jet impinging normally on the wall can remove a large amount of heat over a relatively small surface area. It has been frequently used in cooling the hottest section of a combustion chamber or a turbine blade. Heat transfer rates in case of impinging jets are affected by various parameters like Reynolds number, orifice plate spacing, radial distance from stagnation point, and target plate inclination confinement of the jet, nozzle geometry, and roughness of the target plate.A lot of work is carried out related to impingement on a flat plate or Surface. Hofmann, et al, [1], (2007). Experimentally investigated the flow structure and heat transfer from a single round jet impinging orthogonally on a flat plate. Heat transfer has been studied by means of thermography.

The influence of Z/D and Reynolds number on local heat transfer coefficient has been investigated. Flow structure in a free jet has also been examined, also correlation for heat transfer coefficients have been developed. Vadiraj and prabho, [2], (2008), performed an experimental investigation to study the effect of jet to plate spacing Z/D and Reynolds number Re on the local heat transfer distribution to normally impinging submerged circular air jet on a smooth flat surface. Reynolds number was varied in the range of 12000-28000 and Z/D in the range of 0.5-8. A correlation for the local Nusselt number was developed from the experimental data for two ranges of Z/D $\leq$3 and For Z/D$\geq$ 4. Tadhg and Darina, [3], (2007), investigated the heat transfer distribution from a heated flat plate under impinging air jet with Reynolds number from 10000 to 30000 and Z/D =0.5 to 8. Results shows that at low nozzle to impingement surface spacing, Z/D <2, mean heat transfer distribution in the radial direction exhibits secondary peaks. The peak value of Nusselt number was influenced more by velocity fluctuations normal to the surface than by fluctuations parallel with the surface; this is consistent with the direction of the maximum temperature gradient.

Attalla and Salem,2013**,** [4**],** studied experimentally the effect of nozzle geometry on local and average heat transfer distribution in unconfined air jet impingement on a flat plate, the experiments had been conducted with different of exit Reynolds number. Re was in the range of 6000$\leq$Re$\leq$40000 and plate surface spacing to nozzle diameter, Z/D, in the range of 1$\leq$H/D$\leq$6. An infrared thermography camera was used to record the temperature distribution from isotherms on a uniformly heated impingement surface. With impinging jets, some scientists have used modified surfaces to increase the heat transfer; they have used surface roughness, attached ribs and detached ribs. It can be concluded that in all such situations, these techniques enhance heat transfer. Hence the following review is conducted:

Gau and Lee, 2000, [5], applied rectangular and triangular ribs on the impingement wall. They reported that a higher heat transfer coefficient could be obtained using triangular ribs encouraged the jet to flow smoothly to the wall and generate vortexes

behind the ribs. Also, they varied the ratio of the rib height and nozzle width and varied the rib pitch. It was demonstrated that a lower ratio of rib height to nozzle width provided higher heat transfer. Hansen and Webb, 1993, [6] performed experiments to characterize heat transfer to a normally impinging air jet from surfaces modified with arrays of fin-type extension. Heat transfer enhancement for six fin geometries was evaluated by comparison with results for a smooth, flat surface. Two nozzle sizes with variable Reynolds numbers and nozzle to plate spacing results are reported. The enhancement of heat transfer is measured by calculating the effectiveness for each fin plate, compared to flat surface.

The fin type dependence of Nu as a function of Re was found to be as a result of variations in the turbulence level, fluid velocity, and percentage of total surface area exposed to normal, oblique and parallel flow. For modified surfaces the system effectiveness decreases monotonically with increasing nozzle to plate distance in contrast to the smooth surface behavior. Nakod et al, [7]**,** performed experiments for the effect of the finned (rough) surface on the local heat transfer coefficients between the impinging circular air jet and flat plate. Reynolds number was varied between 6500 and 28000 based on the nozzle exit condition and jet to plate spacing between 0.5 to 7 times that of the nozzle diameter. Thermal infrared imaging technique was used for measurement of local temperature distribution on the flat plate. The fins used were in the form of cubes of 2 *mm* size spaced at a pitch of 5 *mm* on the target plate and hexagonal prism of side 2.04mm and height of 2mm spaced at pitch of 7.5mm. The finned surface had an increased heat transfer coefficient from the target plate, by about 24 to 77% at the base surface depending on the shape of fin, nozzle plate spacing and Reynolds number, in the range studied. The increase in the heat transfer coefficient for finned surface is because of the increase in the swirl i.e. superposition of tangential velocity component into the axial flow, which affect the turbulence characteristics of the flow and decrease the heat transfer coefficient at the top of fin because of the increase in the heat transfer area.

Vadiraj and Prabhu [8], carried experimental investigation is carried out to study the heat transfer enhancement from a flat surface with axisymmetric detached rib-roughness due to normal impingement of circular air jet. A single jet from nozzle of length-to-diameter ratio (l/d) of 83 was chosen. Effect of rib width (w), rib height (e), pitch between the ribs (p), location of the first rib from the stagnation point and clearance under the rib (c) on the local heat transfer distribution was studied. Local heat transfer distribution on the impingement surface was investigated for jet-to-plate distances (z/d) varying from 0.5 to 6 using thermal infrared camera. Turbulence intensity using hot-wire anemometer and wall static pressure measurements were reported for the rib configuration in which maximum heat transfer was observed. Contrary to the results of smooth surface, there was a continuous increase in the heat transfer coefficient from the stagnation point in the stagnation region. This trend is well substantiated by the flow distribution in this region. The ratio of average Nusselt numbers of ribbed and smooth surface was seen to increase with Reynolds number.

The foregoing studies done mainly on slot nozzle type indicate that significant enhancement in jet impingement heat transfer may be achieved with ribbed surfaces.

The present study serves to further investigate this potential and the mechanisms of enhancement. An experimental investigation is reported of heat transfer to axisymmetric impinging air jet from a round orifice for heated surfaces modified with ribs. Heat transfer enhancement is evaluated by comparing the modified surface results to those obtained for smooth, flat surface.

2. Experimental Apparatus

An experimental rig is build and used to study the characterize heat transfer to a normally impinging air jet from surfaces modified with ribs. Air impinge velocity is to be varied in the range 18.4-36 m/s from round orifice of different diameters of (5, 12, 20 mm) with different distances (Z/D) in the range of 4-10 between the orifice and the target plate. Different configurations of modified flat surfaces in form of ribs are studied. Used shapes are rectangular ribs and circular ribs.

The test setup which was used in this work is built up in the workshop of the engineering college at the University of Al-Mustansiriayah. The experiments were conducted in the post-graduate laboratory of the department of mechanical engineering. Fig.1 is a photo picture of the experimental rig and its components. The test rig is designed and manufactured to fulfil the requirements of the test system for a smooth flat surface and modified surface with different configurations of ribs, Set up with an infrared sensitive camera for temperature measurements consists mainly of air blower of (6 m^3/min) capacity, pipe with (50 mm) diameter, a cap fitted at pipe end at which variable orifice diameters can be fixed.

The velocity range is controlled by using a bypass valve fixed near the pipe inlet. A target plate of 30×30 cm^2 steel is fitted at the test section at which the air impinges on it. A constant heat flux from heater wire of (23 Ω) resistance is used to heat the target plate. A Duralumin Alloy plate 0.6 mm in thickness) is placed between the steel plate and the heater to ensure a uniform distribution of the heat within the target plate.

To ensure a reliable thermal coupling and heat dissipation, a Non-Silicon heat transfer compound (Zinc Oxide and C7-C9 Branched alkyl esters) is used between steel and Duralumin Alloy plates and heater as a heat sink. 9 cm thickness polyurethane foam layer is used to reduce the heat losses due to conduction from the lower surface of heated plate. Two thermocouples type-K are fitted on the heated target plate center and plate edge respectively. These thermocouples are used to check the accuracy of thermal infrared image. This is done after making the thermocouple calibration. A high percentage of accuracy is noticed within 95-98%. This high accuracy ensures that thermal infrared images will give an excellent indication of temperature distribution on the flat plate.

A procedure is made for the ribbed surface with five thermocouples fitted in transverse and longitudinal directions with distance of 3 cm pitch on the ribbed surface. Additional two thermocouples are used to calculate the heat losses due to conduction from the lower surface of heated plate. All thermocouples inserted through drilled holes from the bottom of the test section and welded by epoxy resin to the heated plate. A single thermocouple is used to measure the ambient temperature. A wooden box is used to retain the plate assembly forming the test section. Fig.2 shows test section details. An

adjustable base is used to control the height of the test section according to the target plate to orifice diameter spacing (Z/D).

Two types of heated target plates were designed and manufactured in the present work; each plate made of steel 30×30 cm^2 is fitted at the test section. The thickness of the first smooth, flat target plate are 0.4 mm. The second target plate, used in the proposed study consists of different configurations of modified surfaces in the form of ribs (roughened) surface with a thickness of 1 mm such as: rectangular and circular ribs. Note that, the ribs were designed with different sizes spaced at different pitches. Fig.3shows Photographs of target plates fitted at the test section: (a) Smooth flat surface (b) rectangular rib surface.

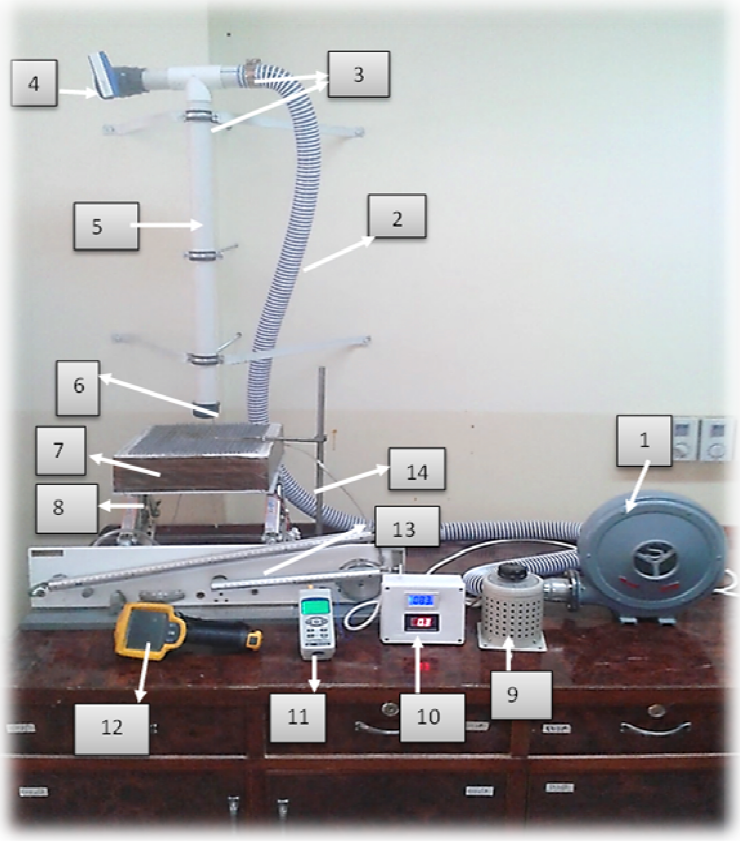

1-Air Blower 2-Plastic Hose 3-Holder 4-Bypass Valve 5-P.V.C Pipe 6-Orifice
7- Test Section 8-Adjustable Base 9-Variac 10- LCD Display 11-Readers
12-Infrared imaging technique 13-Manometer
14- Travers

Figure 1. Experimental test rig

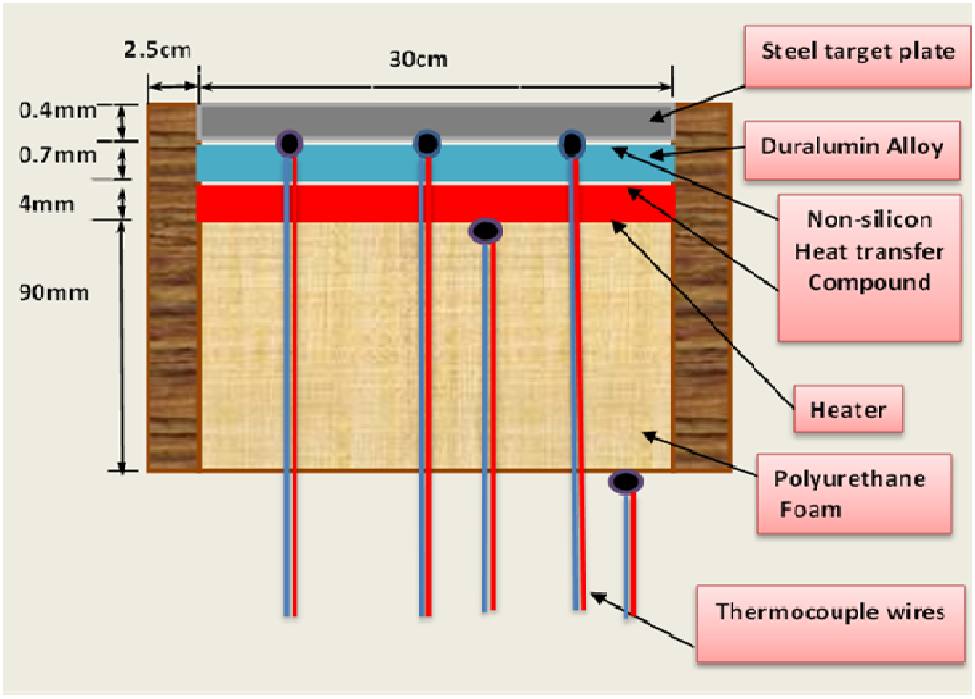

Figure 2. Test section

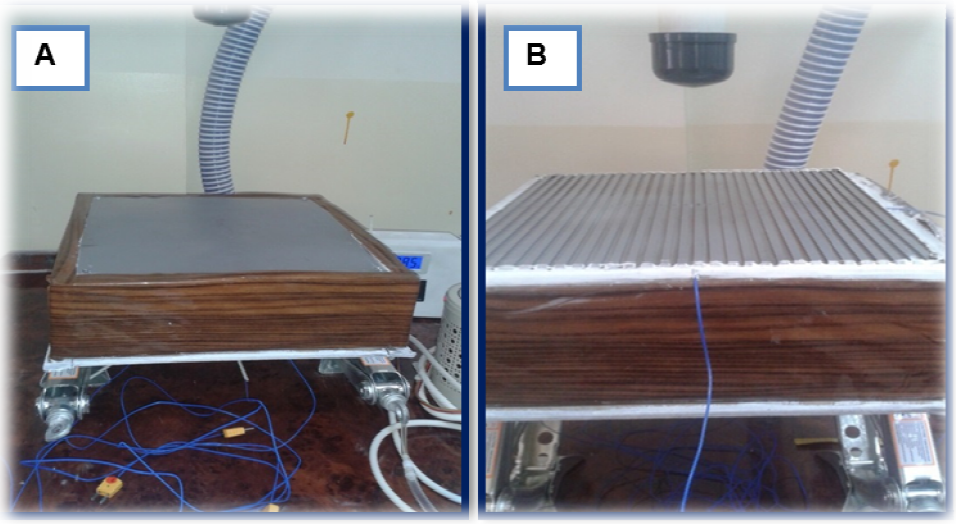

Figure 3. Photographs of a target plate fitted at test section: (A) Smooth flat surface

(B) Rectangular rib surface

Three arrangements of rectangular ribbed surfaces were designed and manufacturedusing a milling machine; each one consists of a steel square target plate of 30×30 cm^2 and 1 mm in thickness. Each plate have a number of 30cmlongitudinal rib elements distributed parallel to each other along the surface with different sizes spaced at different pitches on the target plate. Fig.4(a) shows a schematic diagram of rectangular ribbed surface. Two different circular ribs surfaces each one have a number of 30 cm long rib elements with circular cross section having deferent rib

pitches of 10 and 5mm with different sizes which are mounted and glued in parallel on the steel surface. Fig. 4(b) shows a schematic diagram of circular ribbed surface.Range of parameters and rib geometry is given below in Table 1 and Table 2.

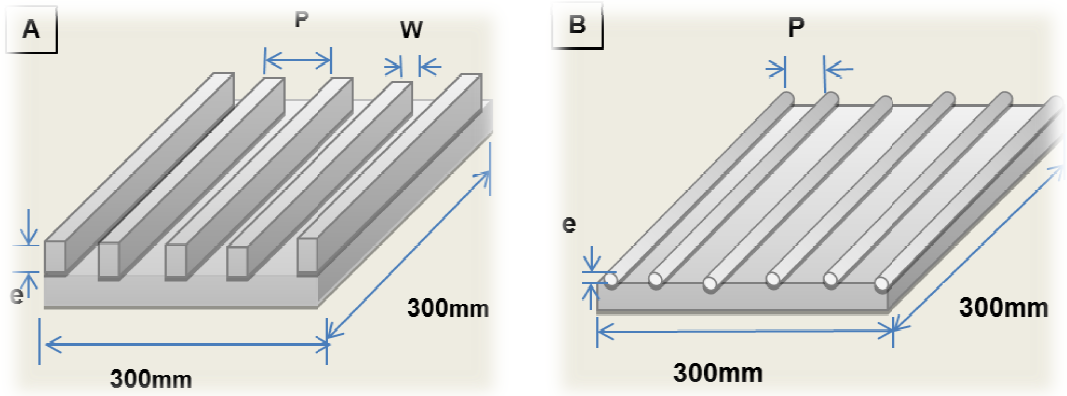

A schematic diagram of rectangular ribbed surface A schematic diagram of circular ribbed surface

Figure 4. The test plate

Table (1): Range of parameters of rectangular ribbed surface

Case	Rib width (w)	Rib height (e)	Rib pitch (p)	p/e	p/w	Number of ribs
Case 1	6mm	2mm	10mm	5	1.67	30
Case 2	3mm	2mm	7.5mm	3.75	2.5	45
Case 3	6mm	3mm	10mm	3.34	1.67	30

Table (2): Range of parameters of circular ribs surface

Case	Rib height (e)	Rib pitch(p)	p/e	Number of ribs
Case 1	2mm	10mm	5	30
Case 2	2mm	5mm	2.5	50

A handheld thermal imager (Ti32) is used to collect the local temperature distribution over a target plate. It is calibrated by measured the temperature of the target surface using calibrated thermocouple type K fixed in target plate, in same time the temperature is measured by thermal imager . The target plate surface is heated by hot main stream. The temperatures obtained by both measuring way is recorded during the heating process until achieving a steady state condition. Infrared camera reads the temperature of the target plate depending on the emissivity value of the surface of the target plate. Due to the emissivity of the test surface the temperature recorded by IR thermal image is adjusted until both reading temperatures are matched.

3. Theory

The total input power that generated from the heater wires is calculated as follows:

$$Q_{input} = IV \qquad (1)$$

The net heat transfer by convection is calculated as follows:

$$Q_{conv.} = Q_{input} - \sum Q_{losses} \qquad (2)$$

$$Q_{conv.} = Q_{input} - Q_{rad.} - Q_{cond.} \qquad (3)$$

The heat transfer per unit surface through convection was first described by Newton's law of cooling. It can be expressed as:

$$Q_{conv.} = hA_s(T_s - T_f) \qquad (4)$$

The constant heat flux on the plate face is calculated according to following equation:

$$q''_{conv.} = \frac{Q_{conv.}}{A_s} \qquad (5)$$

Equation (5) is used to calculate the heat flux in case of a flat plate or base surface.
In case of ribbed surface the heat flux is calculated as from equation

$$q''_{conv.} = \frac{Q_{conv.}}{(A_s + Arib)} \qquad (6)$$

The local heat transfer coefficient is evaluated using the following equation:

$$h = \frac{q''}{T_s - T_f} \qquad (7)$$

Both, the average and local heat transfer coefficient are related by an expression of the form:

$$h_{avg} = \frac{1}{A_s}\int_{A_s} h dA_s \qquad (8)$$

For the flow over a target plate h varies only with the distance, so that equation (8) reduces to:

$$h_{avg} = \frac{1}{L_s}\int_0^{L_s} h dx \qquad (9)$$

The ratio of conductive thermal resistance to the convective thermal resistance of the fluid is known as the Nusselt number, is calculated on the basis of heat transfer coefficient:

$$Nu = \frac{hD}{K_j} \qquad (10)$$

4. Results and Discussions

The experimental evaluation has been carried out for the velocity distributions, heat transfer coefficients, temperature distributions at different Z/D values for smooth flat plate and modified surfaces with ribs.

4.1 Free jet Velocity distribution measurements:

The flow structure of the jet from the orifice is investigated by measuring the velocity distribution in a free jet impinging from orifices of different sizes at different radial positions from the jet centreline at the same axial distance. The flow structure and velocity profile at orifice exit in free jet are measured using the total tube and traverse mechanism .The process is accomplished after removing the target plate to prevent any impact with the jet.Fig.5 presents the flow structure at jet exit is non-dimensionally plotted with the axial positions of (y/D = 0, 2, 4, 6 and 8)for the orifice sizes 20mm for maximum velocity, where U/U_j represents the non-dimensional velocity taken relative to the jet exit. It shows that at small axial distances from the orifice i.e. near orifice exit the velocities are almost constant and equal to jet exit velocity except the regions near the orifice edges, at these positions the air jet velocity decays in a high rate reaching zero at a small distances beyond the orifice edge. It can be observed that the further axial distance from the orifice exit is the less velocity is occurred at that point. In contrast, if the distance is far away from the orifice, the velocity will be widely distributed like a bell shape. Therefore, the velocity distribution is spread extensively at the further distance from the orifice with lower velocity.

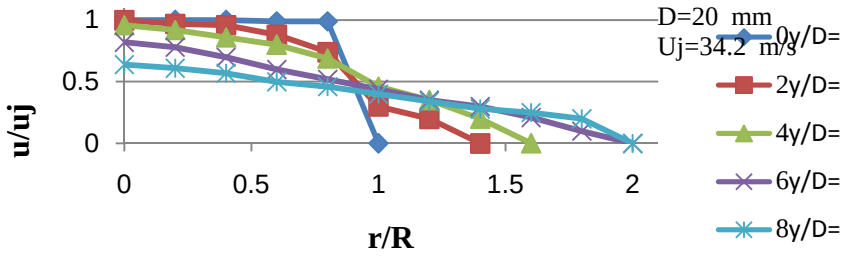

Figure 5. Flow structure at jet exit (D=20 mm, Uj=34.2 m/s)

4.2 Boundary layer profile on a smooth flat plate and ribbed surfaces measurement

Boundary layer profile is measured at different axial positions from the orifice plate, using a total tube designed for these measurements. Three dimensional traversing mechanism displacements are in both the axial direction, and horizontally in each axial position from orifice plate is used to traverse the total tube for measuring the dynamic head of the impinging jet. Fig. 6represent the boundary layer distribution of air jet on the smooth target plate for orifice -to-plate distance Z/D=6 and for highest velocity of tested velocities for each of orifice diameter D= 20mm at different radial positions starting from the stagnation point (X) on a flat plate and moving outward in radial direction. It is noticeable that the boundary layer has the maximum value of velocity near the stagnation point. At this point, the boundary layer thickness is relatively small. On the other hand, the highest thickness of the boundary layer is observed at point's where wall jet velocities start to diminish.

The boundary layer thickness increases away from plate centre with reduction in wall jet velocity. This is because of the reduction in wall jet momentum described by ordinary boundary layer behaviour and development of shear stresses with the plate surface Velocity distribution in the wall jet regions are with the same trend of experimental measurements for different authors such as Hofmann,et.al [1] and Vachirakornwattana[10]. For ribbed surfaces the velocity distribution within the boundary layer in wall jet region is measured for both in the longitudinal and transverse direction. The preface of the ribs will enforce the air to flow through the cavity between the ribs (in longitudinal direction), then the velocity distribution is seems high in value and almost nearly with same values as a flat plate.

In transverse direction the flow structure is affected by rib height and rib pitch, the flow will continue with fluctuations and resistance causing lower velocities .Wall jet velocity measurements for smooth and ribbed surfaces are shown in Fig.7 for orifice diameter D=20 mm. Measurements show that wall jet velocity for the flat plate always higher than that for the case of ribbed surfaces with different rib sizes and pitches, noticing that the wall jet measurement of ribbed surfaces are taken on the rib surface not within the channel passages. (These results are taken for transverse directions only).

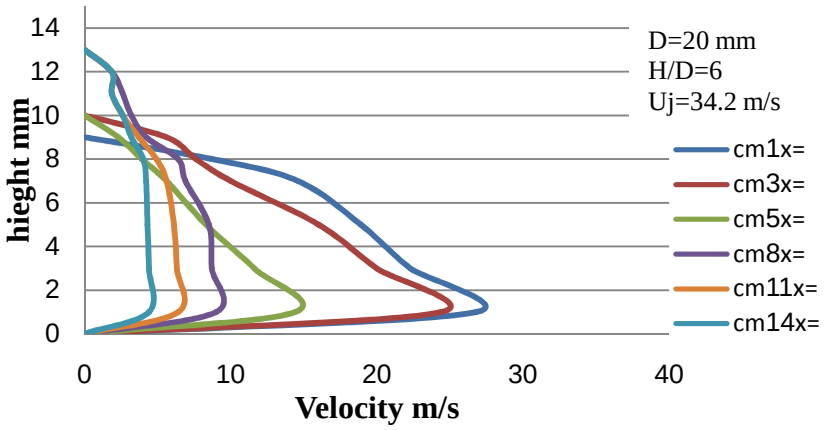

Figure 6. Boundary layer profile on asmooth plate surface at different radial positions (D=20 mm, U_j =34.2 m/s, Z/D=6)

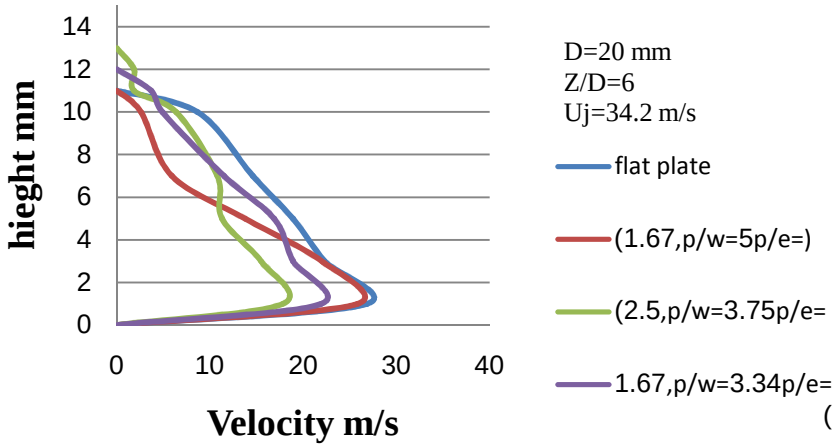

Figure **7.** Boundary layer profile on a smooth plate surface and rectangular ribbed surface at radial positions starting from the stagnation point X=1cm (D=20 mm, U_J=34.2 m/s, Z/D=6)

4.3 Smooth flat plate

Fig. 8(a) shows an example of the thermal image that has been obtained at the distance between the orifice and flat plate at Z/D=4 for D=12mm and for highest jet velocity tested (U_J=35 m/s), a constant heat input of 48 W has been supplied to the plate. It is observed that, the temperature distributions due to the impinging jets are perfectly symmetric around the stagnation point except for the far field of the region of impingement, this is due to decrease of cooling degree .Fig. 8(b) show the local temperature distribution along the horizontal line from the stagnation point on the target plate, the variation of temperature is plotted with the radial distance from the plate center (x), because of the axisymmetric of the profile.

As can been seen from Fig.9(a), temperature distribution shows a minimum value at the stagnation point and increased with the radial distance from the plate center this is due to decrease of cooling degree. Fig. 9 shows the local distribution of the heat transfer coefficient -based on temperature distribution- along the horizontal line through the stagnation point for D=20 mm, Z/D=6and U_J=34.2 m/s.As can been seen from Fig., the heat transfer coefficient shows a maximum value at the stagnation point and decreased with the radial distance from the plate center. Examining the effect of different height to orifice diameter ratio Z/D shows that optimum ZD values which gives the highest $h_{stag.}$and$h_{avg.}$is Z/D=6.

Fig.10 shows a graphical representation of average heat transfer coefficients and its variation with je velocity and Z/D for D=20 mm. Other orifice sizes have the same trend. This is in agreement with other researcher results as Hofmann,et al [1]local heat transfer coefficients distribution for different jet velocities and Z/D values presented as Nusselt number distribution is shown in Fig.11 for D=20 mm. The maximum obtained value of Nusselt number is found at stagnation point and decreased with radial distance from the plate center. This isn't surprising since fluid is being convicted away from the stagnation region rapidly and loses its turbulence kinetic energy. Other orifice diameters are tested in the same manner and show the same trend for various tested parameters.

The following equation gives an empirical correlation found from experimental results for 64 tests on different orifices size (5, 12 and 20 mm);

$$Nu_{stag} = 0.811 \ \mathrm{Re}^{0.54} (Z/D)^{-0.1} \quad (11)$$

Fig.12(a) and (b) shows the representation of the data represented by equation (11) and comparison with experimental results given by of Attalla and Salem. [4]. the correlation is found to fit the present experimental data with 10-15%, while its difference with of Attalla and Salem [4] Data is within 10-20%.

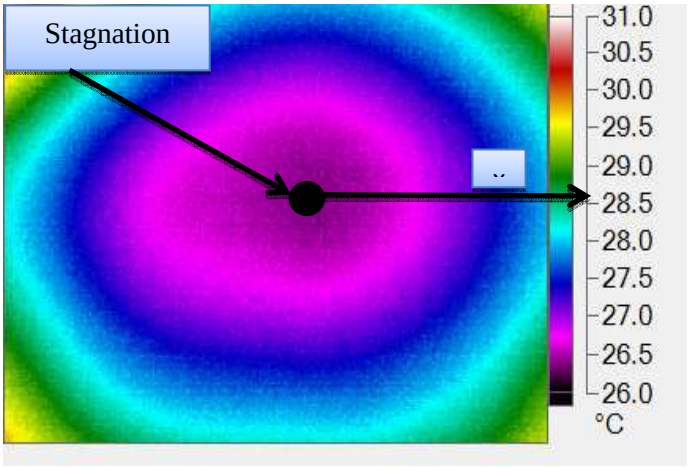

(a)

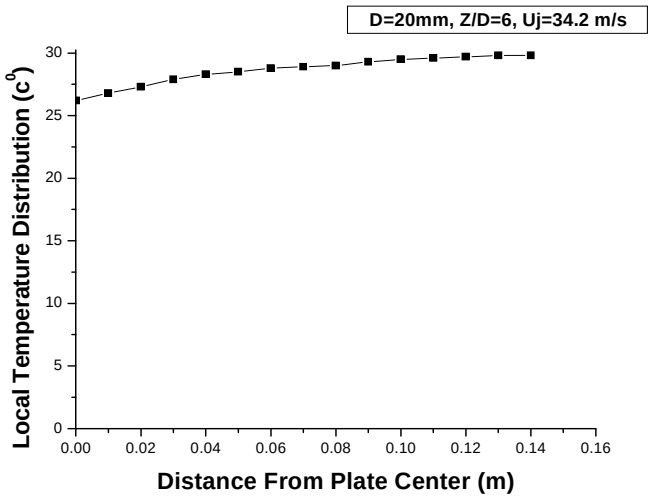

(b)

Figure 8. (a) Thermal image; (b) Local temperature distribution

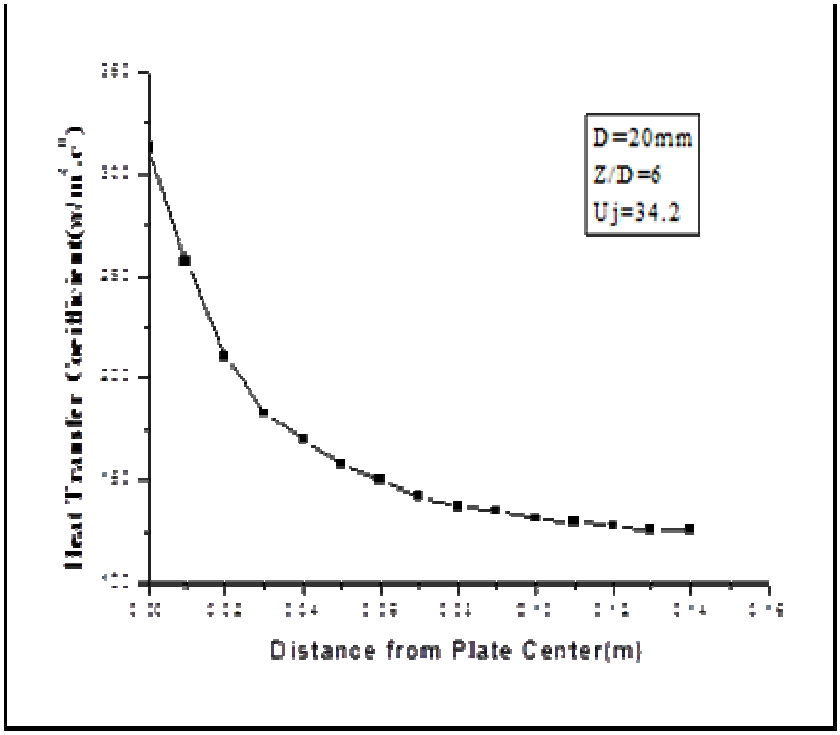

Figure 9. Radial heat transfer coefficient distribution at (D=20mm, Uj = 34.2 m/s, Z/D=6)

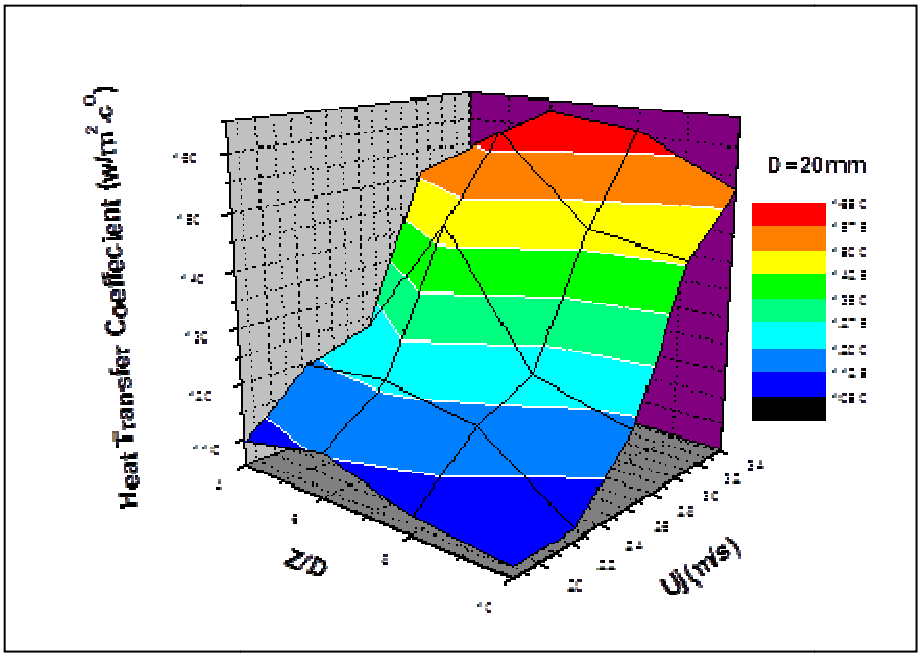

Figure 10. Graphical representation of average heat transfer coefficient, D=20mm

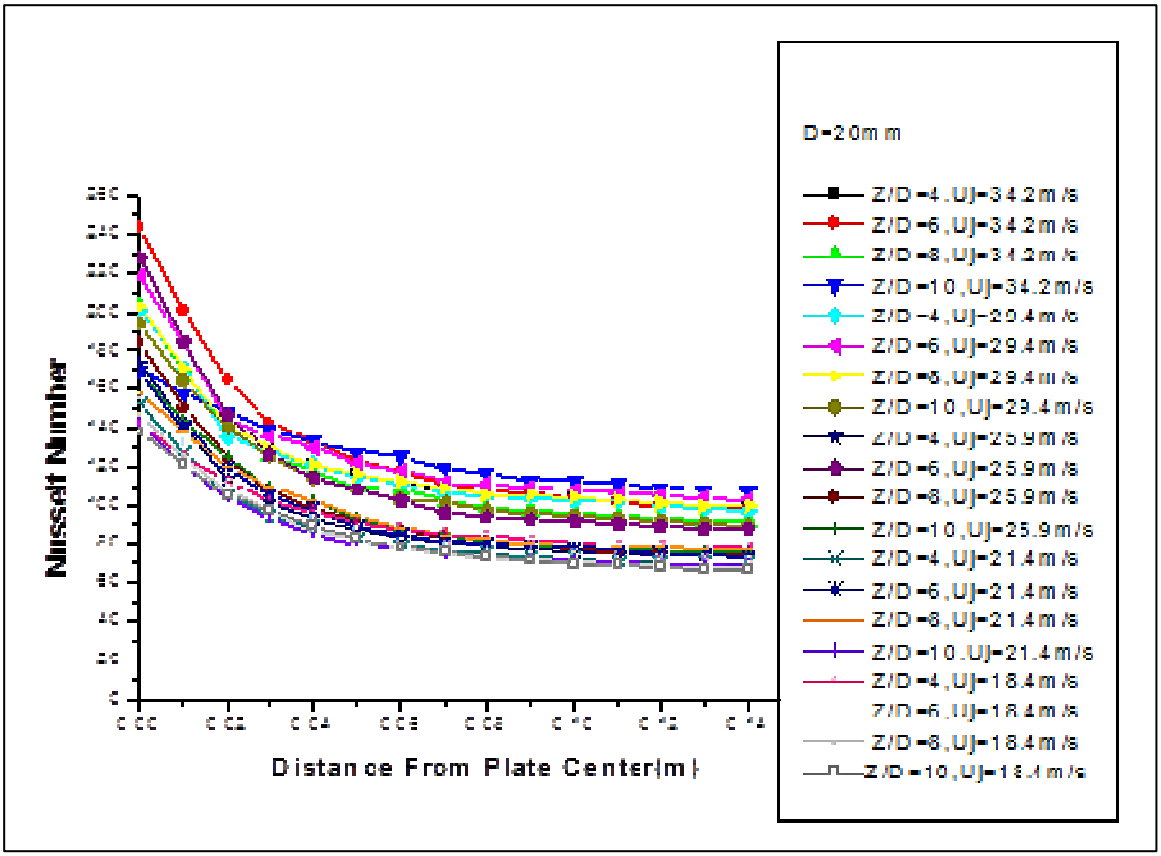

Figure 11. Local Nusselt number distribution, D=20mm at (different Z/D and Uj values)

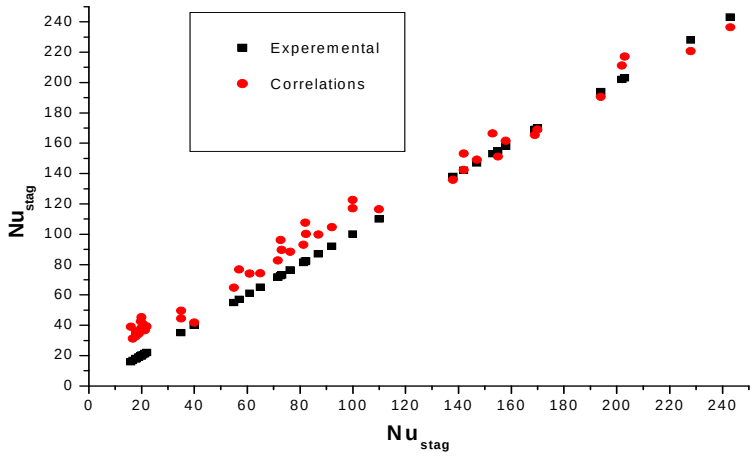

(a)

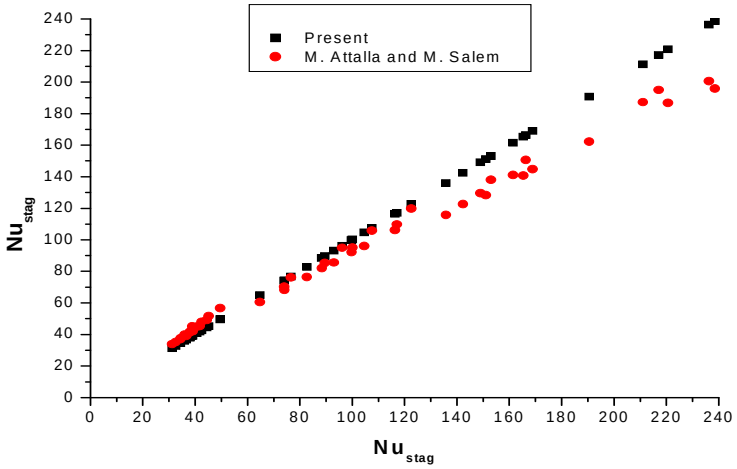

(b)

Figure 12. (a) Nustag from experimental measurements values its values as a predicted from correlation; (b) Present experimental results values that by reference [4]

4.4 Rectangular ribbed surfaces

Fig.13 shows an example of the thermal image that has been obtained on the target plate for the distance ratio between the orifice and rectangular ribbed plate Z/D=6 for D=5 mm and for highest tested velocity U_J=36 m/s. The Fig. shows that the transverse direction is the horizontal line through the stagnation point and longitudinal direction is the normal to transverse directions of the ribs. It is observed that, the temperature distributions due to the protrusion of the ribs are different from that for a flat plate due to different flow field. Such difference in temperature distribution is attributed to vortex generated and separation of streamlines of flow on the rib, in addition to lower velocities of air impinged within the ribs. This trend is similar to that observed by C. Gau and L. C. Lee [5]. Temperature distribution on the rectangular ribbed plate at T_∞=21.3 C^O and a flat plate at T_∞=14.7 C^O is shown in Fig.14 for U_J=36 m/s and Z/D=6 at constant heat input of 48W has been supplied to the ribbed and flat plate.

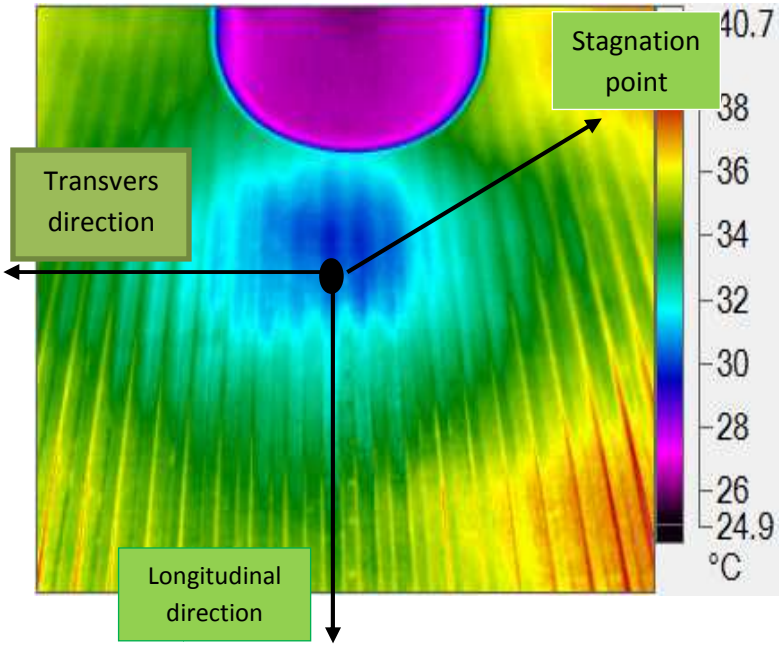

Figure 13. An Examples of infrared measurement of an impingement on rectangular ribbed surface for D=5mm and Uj=36 m/s, Z/D=6

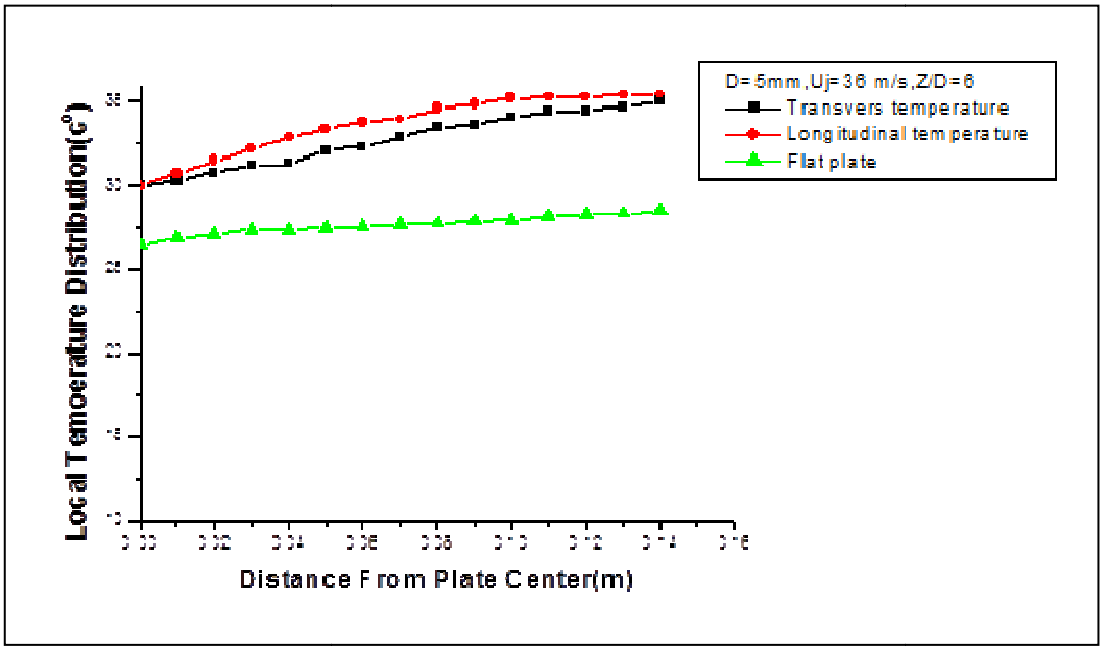

Figure 14. Local temperature distribution on the flat plate at T_{∞}=14.6C^{O} and rectangular ribbed plate at T=21.3C^{O} (U_J=35 m/s, Z/D=6).

Fig. 15 and 16 give examples of the comparison of the local heat transfer coefficient for smooth flat plate with the longitudinal and transverse directions of the ribs on the basis of the base area as a flat plate and the basis of the modified surface area (the sum of the base plate plus the surface of the ribs) for rectangular ribbed surface with (p/e=5,p/w =1.67) for D=20mm at orifice to plate distance Z/D=8 and for highest tested velocity (U_J=34.2 m/s). It is observed that there is an increase in the heat transfer

coefficient for rectangular ribbed surface in longitudinal and transverse directions as compared to smooth flat plate and then there is an enhancement in both directions, attributed to the function of ribs that make the flow turbulent, which results in an enhancement of the heat transfer. The heat transfer results for rectangular ribbed surface show higher Nusslet number compared to smooth flat plate as base area (flat plate area only). From Fig. above the results calculated on both cases; on the basis of the base area as a flat plate and the basis of the modified surface area (the sum of the base plate plus the surface of the ribs) as an example. Other results are calculated for the base area only in order to show the enhancement heat transfer coefficient, also, due to the fact that the variation in longitudinal and transverse direction is within a limited range and in order to give a general behavior of enhancement in heat transfer, the average value for the whole plate in both longitudinal and transverse directions for all results is calculated as follows:

$$h_{avg} = \frac{(\text{h longitudinal+ h transvers})}{2} \quad (12)$$

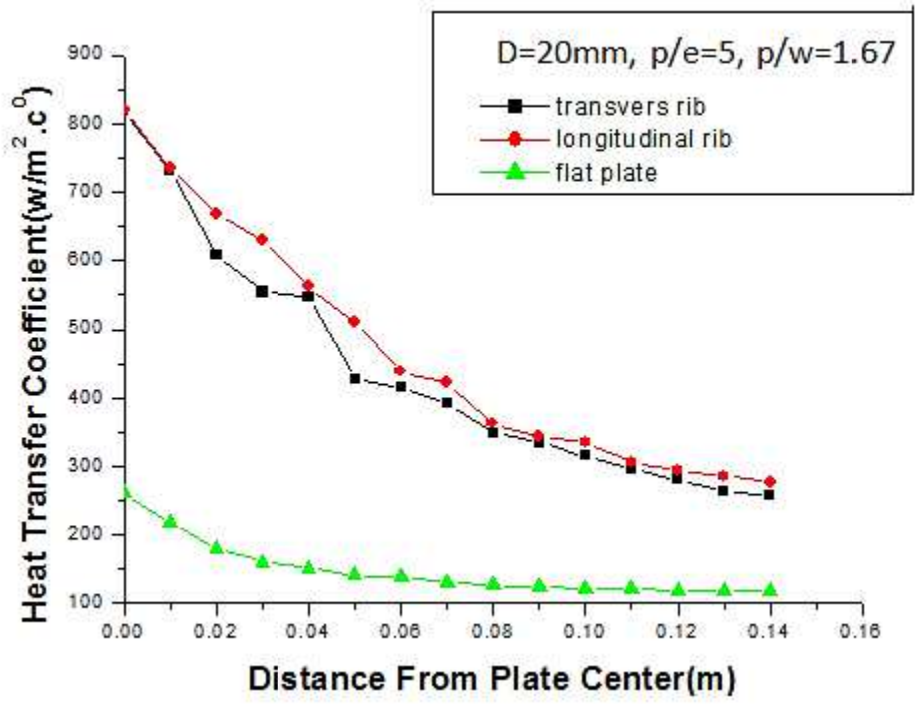

Figure 15. Heat transfer coefficient distribution calculated on flat area as a base for (D=20mm, Uj=34.2m/s, Z/d=8, p/e=5,p/w =1.67)

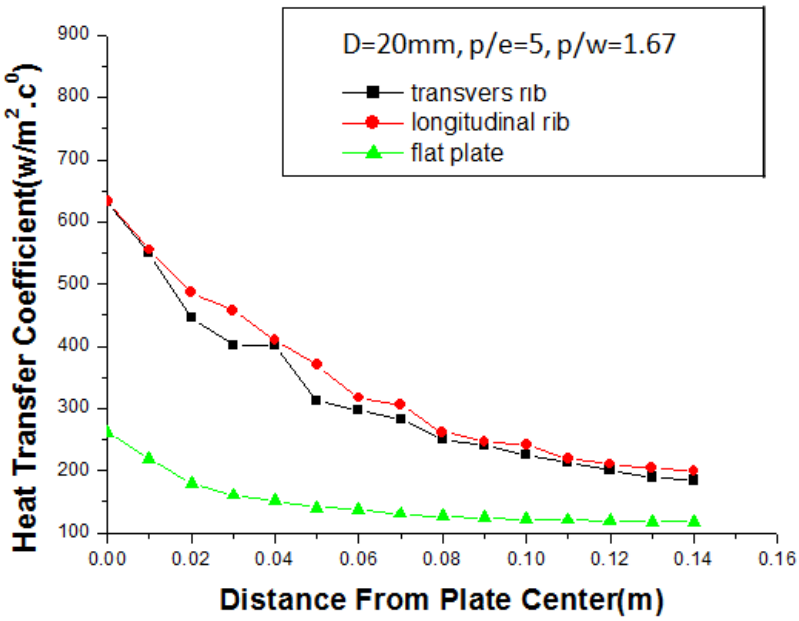

Figure 16. Heat transfer coefficient distribution calculated on modified area for (D=20mm, Z/d=8, Uj=34.2m/s, p/e=5,p/w=1.67)

Fig.17, 18, and 19 show the radial profiles of the experimental Nusslet number for all arrangement of rectangular ribbed surfaces and smooth flat plate for orifice diameter D = 20 mm, orthogonal distance to diameter ratio Z/D= 8 and jet velocity =34.2m/s It reveals that the rectangular ribbed surfaces with three arrangements result in enhanced Nusselt number, as compared to the smooth flat surface, other orifice sizes have the same trend. Gaw and. Lee [5] observed same behavior of the enhancement in Nusslet number when they used rectangular ribs on the impingement wall. They reported that for impingement cooling over a rib –roughened wall, the protrusion of the ribs has the effect of promoting turbulence in the wall jet and generate vortexes behind the ribs. In addition, the wall jet passing through the cavity can separate from the rib, and recirculate inside the cavity; therefore, a significant enhancement occurs in heat transferred along the ribbed wall.

The increase in the heat transfer on the rectangular ribbed surface is because of the increase in the swirl i.e. superposition of tangential velocity component onto the axial flow, which affects the turbulence characteristics of the flow. As shown in Fig. the maximum Nusselt number is obtained in the stagnation point decreases monotonically in the radial direction. Different orthogonal distance to diameter ratio (Z/D) are tested and its local Nusslet number distribution in radial direction is shown with highest $Nu_{stag}$is measured at Z/D=8, this attributed to higher turbulence intensity in this case. The Fig. shows that stagnation and average Nusslet number for Z/D=8 with Three cases for ribbed plate are given in Table 3. Rib arrangement constitutes p/e(rib pitch-to rib height ratio), p/w (rib pitch–to width ratio) and number of ribs.

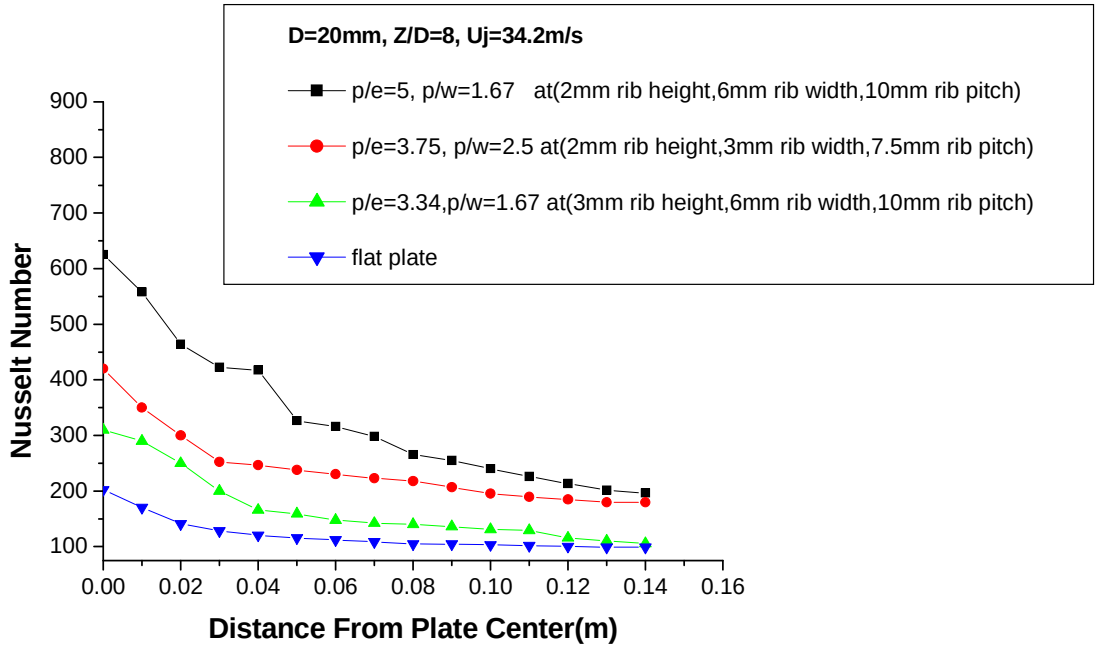

Figure 17. Radial profile of the Nusselt Number for all rectangular ribbed surface and Smooth flat plate for (D=20mm, Uj=34.2m/s Z/d=8)

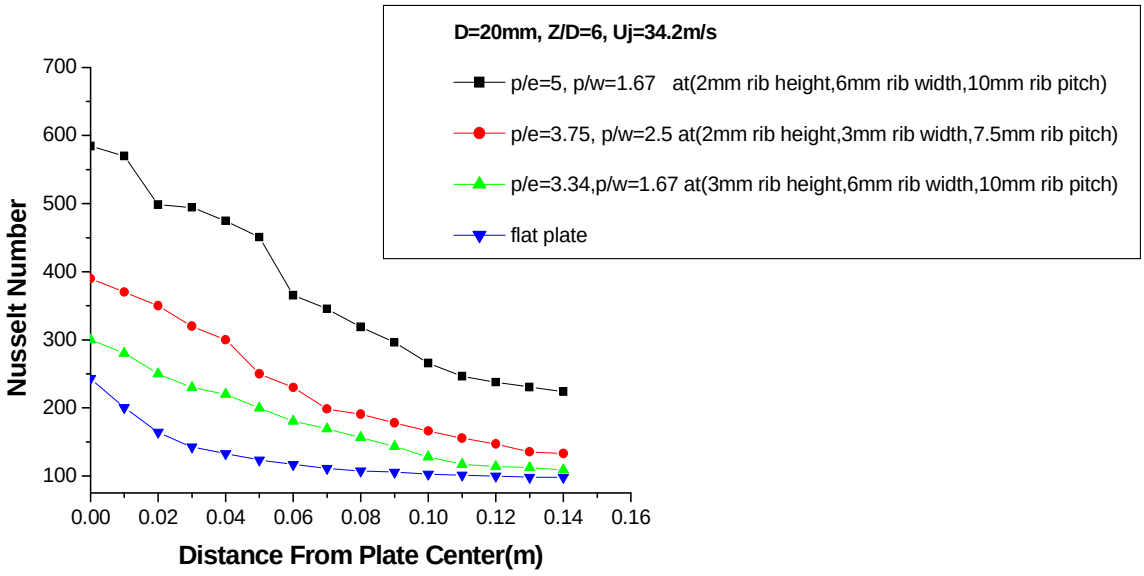

Figure 18. Radial profile of the Nusselt Number for all rectangular ribbed surface and Smooth flat plate for (D=20mm, Uj=34.2m/s Z/d=6)

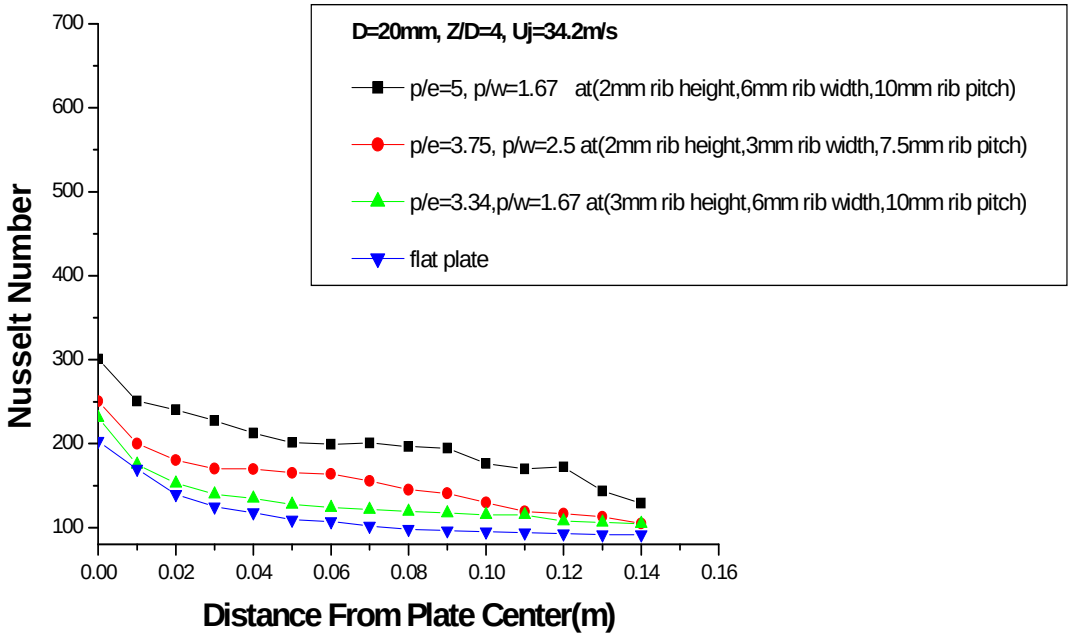

Figure19. Radial profile of the Nusselt Number for all rectangular ribbed surface and Smooth flat plate for (D=20mm, Uj=34.2m/s Z/d=4)

Table (3) stagnation and average Nusselt number for D=20mm, Z/D=8,Uj=34.2m/s.

cases	Rib arrangement	Nu_{stag}	Nu_{avg}
1	p/e = 5, p/w =1.67, number of ribs is 30	626	370
2	p/e = 3.75, p/w =2.5, number of ribs is 45	366	230
3	p/e=3.34,p/w =1.67, number of ribs is 30	235	196

The case (1) of rectangular ribs of p/e=5, p/w=1.67 with rib height 2mm gives higher in enhancement in heat transfer relative to case (3) of p/e=3.34, p/w=1.67 with rib height 3mm. This can be attributed to higher inertia of air flow between ribs and higher freedom in air flow which gives better air flow which increases heat rates when the rib height is smaller. It can be discussed on the base that vortex formation in case of rectangular ribbed surface with e=3mm is in a higher rate than that in case of rectangular ribbed surface with e=2mm. This vortex means higher air temperature with limited air flow, this reduces heat transfer coefficient, and hence an increase in rib height reduces velocity within the ribs cause a decreases in heat transfer coefficient. Also case (1) of rectangular ribs of(p/e=5, p/w=1.67, 10 mm pitch) gives higher in enhancement in heat transfer relative to case (2) of (p/e=3.75, p/w=2.5, 7.5 mm pitch) keeping height of the rib (e = 2mm) constant .This is due to the fact that when the pitch of the ribs (the cavity between neighboring ribs) increases, the amount and the velocity

of the wall jet penetrating in the cavity are higher This leads to a higher heat transfer in case of p/e=5 than in the case of p/e=3.75. Gau and Lee [5] observed same behavior they found that, when the cavity between neighboring ribs increase, make more intense transport of momentum between the wall jet and cavity flow.

Fig. 20 and 21 presents the effect of orifice diameter on Nusslet number distribution for all arrangements of rectangular ribbed surface in case one of (p/e=5, p/w=1.67) for jet velocities of only the minimum and maximum values for each diameter for Z/D=8. Figures show that the maximum Nusselt number occurs in the stagnation region and decreases with increasing radial distance.

This behavior is noticed for all orifice sizes. Small orifice sizes gives lower heat transfer coefficients, so Nusslet number decreases with decreasing orifice sizes attributed to small momentum of jets of small orifice size, with shorter potential flow core, smaller affected zones of the target plate for both smooth and ribbed plate's gives lower heat transfer rates at stagnation zone and beyond it. Also Figures show that, high air jet velocity gives higher jet momentum which means higher penetration rate whiten the ribs and more ability for turbulence intensity and recirculation inside ribs cavities giving higher heat transfer rates. Low air jet velocities gives smaller effect on heat transfer enhancement within ribs modified regions because of low jet momentum and due to lower Reynolds number the jet is considered as hydrodynamically smooth on ribbed surface(roughness effect is neglected),hence lower heat removal rates is noticed.

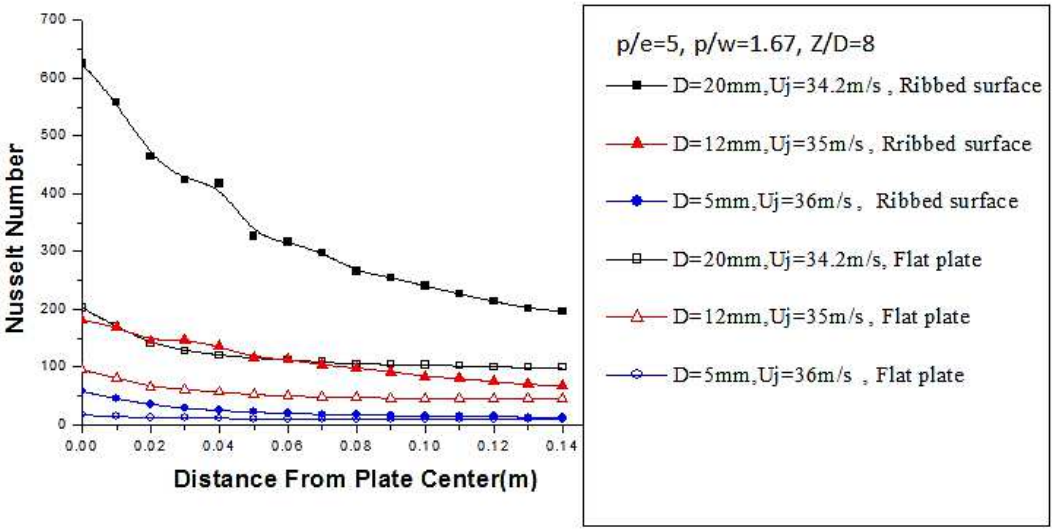

Figure20.Local Nussle number distribution for the case of p/e=5 , p/w=1.67, Z/D=8 at maximum jet velocity for each orifice diameter D=(5,12,20)mm

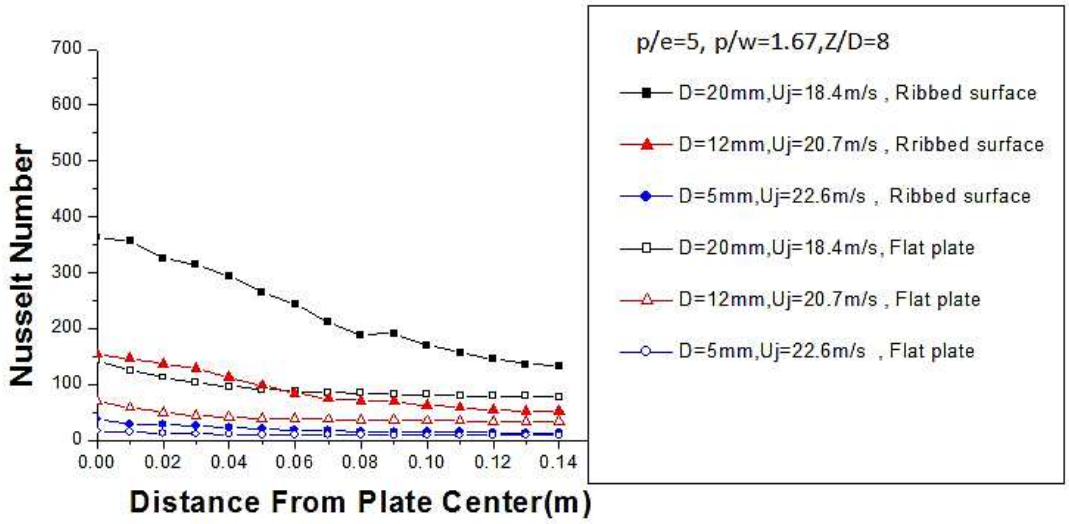

Figure 21.Local Nussle number distribution for the case of p/e=5 , p/w=1.67, Z/D=8 at minimum jet velocity for each orifice diameter D=(5,12,20)

Fig.22, 23, and 24 shows the enhancement ratio factor (*EF*) of the absolute rate of heat transfer coefficient as a function of Reynolds number for all rectangular ribbed surface at Z/D=8 for orifice diameters D= (5, 12, 20) mm. The enhancement ratio factor (*EF*) is the ratio between the average heat transfer coefficient when using the rectangular ribbed surface to the average heat transfer coefficient when using the flat smooth surface, ($h_{avg\ ribbed}$ / $h_{avg\ smooth}$) at the same Reynolds number. Fig. show that, generally, *(EF*) increases with Reynolds number. The enhancement ratio factor (*EF*) is greater than unity for all orifice sizes, indicating an increase in the rate of heat transfer for all rectangular ribbed surface compared with the smooth surface. This was a result of the effect of the turbulence introduced by ribs.

The magnitude of the enhancement, as represented by the enhancement ratio factor (*EF*), was strongly dependent on the rib geometry. The dependence of the enhancement ratio factor (*EF*) on rib type is a function of two factors given for the average heat transfer coefficient dependence (level of turbulence ,fluid velocity) The rectangular ribbed surface with (p/e=5,p/w=1.67) which results in the greatest increase in Nusslet number enhance the heat transfer coefficient at the stagnation point by factor ranging from approximately (2 to 3), The rectangular ribbed surface with (p/e=3.75,p/w=2.5) enhance the heat transfer by factor ranging from approximately (1.5 to 2) and The rectangular ribbed surface with(p/e=3.75,p/w=2.5) enhance the heat transfer by factor ranging from approximately (1.2 to 1.75).

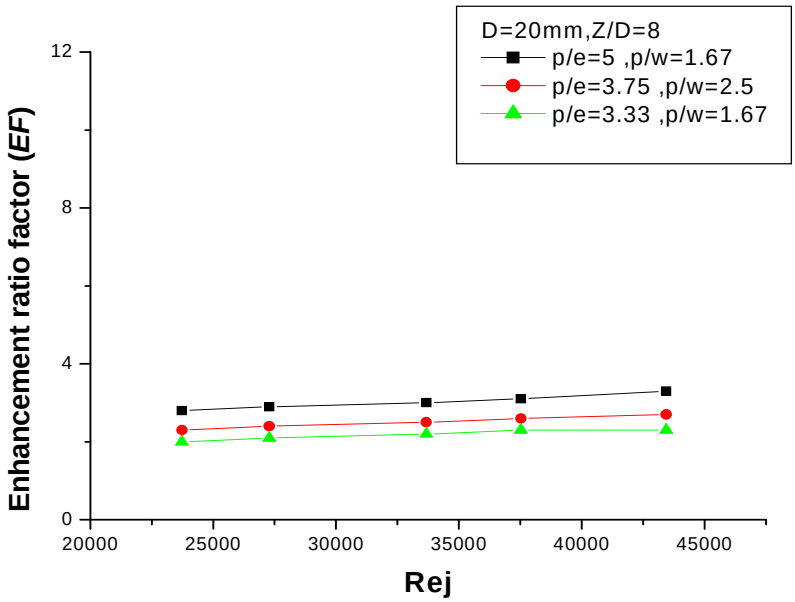

Figure 22. Enhancement ratio factor (EF) as a function of Reynolds number for rectangular ribbed surface for D=20mm,Z/D=8

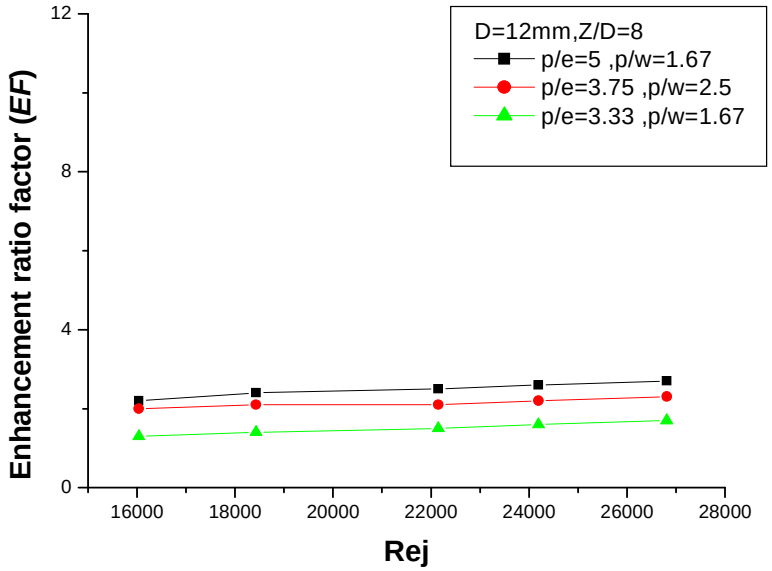

Figure 23. Enhancement ratio factor (EF) as a function of Reynolds number for rectangular ribbed surface for D=12mm,Z/D=8

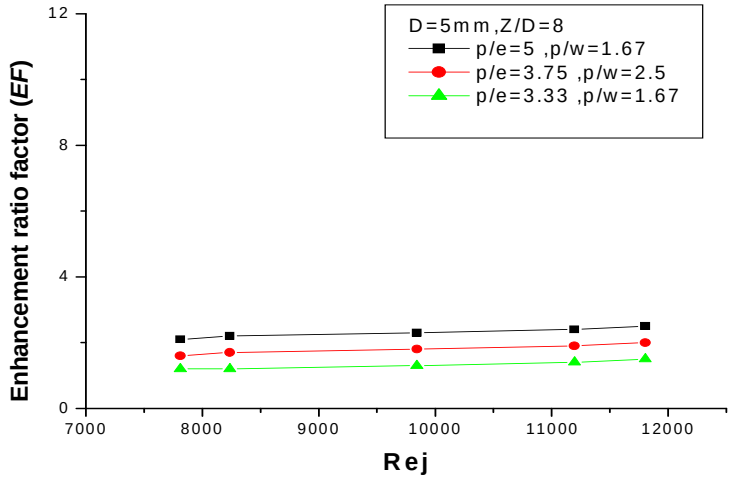

Figure 24. Enhancement ratio factor (EF) as a function of Reynolds number for rectangular ribbed surface for D=5mm,Z/D=8

4.5 Circular ribbed surfaces

Fig. 25 and 26 give the comparison of the Nusselt number for smooth and circular ribbed surfaces at different orifice size and orthogonal distance to diameter ratio Z/D= 8 for jet velocities of the maximum values of the complete set of velocities used in these measurements for each orifice diameter. It reveals that the heat transfer results for circular ribs surface, similar to rectangular ribbed surface, shows an increase in Nusslet number for all orifice size as compared to smooth flat surface. It is also seen that the value of Nusselt number increases with the increase in rib pitch-to-rib height (P/e). It is attributed to that the increase in rib pitch-to-rib height (P/e), the distance between the protrusions increases which results in making more intense transport of momentum between the wall jet and cavity flow This leads to a higher heat transfer around the cavity wall than in the case which have narrow cavity. This is in agreement with other researcher results as Gaw and Lee [5].

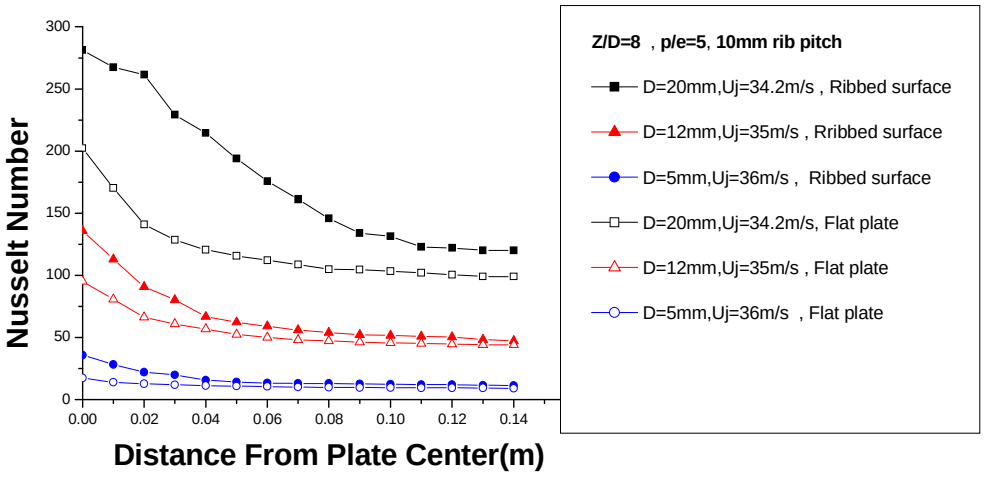

Figure 25. Local Nussle number distribution for the case of circular rib with p/e=5 ,Z/D=8 at maximum jet velocity for each orifice diameter D=(5,12,20)mm

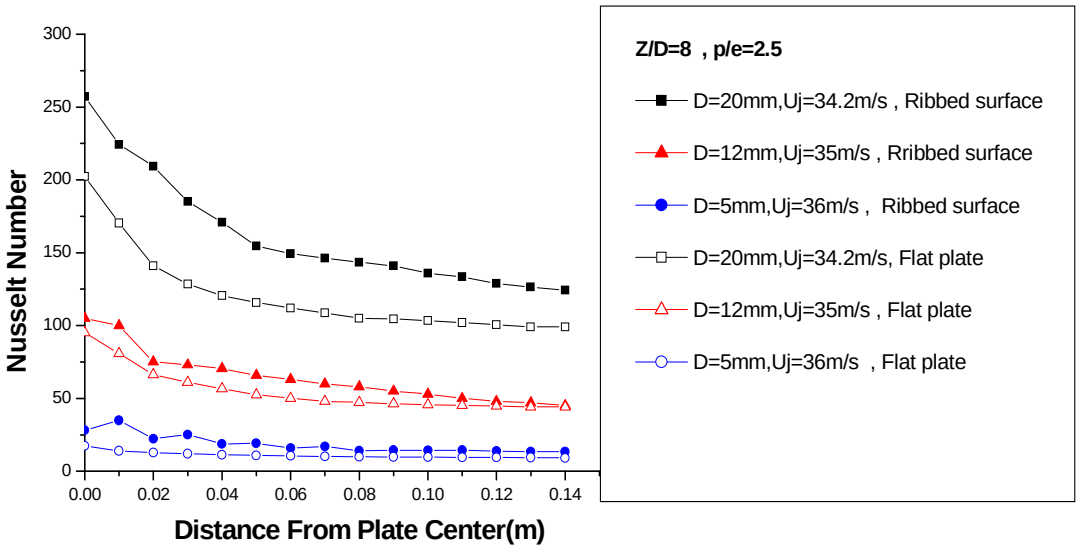

Figure 26. Local Nussle number distribution for the case of circular rib with p/e=2.5 ,Z/D=8 at maximum jet velocity for each orifice diameter D=(5,12,20)mm

5. Conclusions

The conclusions are classified in accordance with the type of target plate.

A- Impingement on a target flat plate.

1. Increasing Reynolds number will lead to increases in the heat transfer at all the radial locations for a given Z/D.
2. The biggest diameter results in a higher heat transfer for the same jet velocity.
3. In all the studied cases, the results show that stagnation point heat transfer coefficient is with the highest values relative to the other points.
4. The optimum value of Z/D is 6 for all orifice sizes (5, 12, 20mm).

B- Impingement on ribs or modified surfaces:

1. The ribbed surfaces with five arrangements increase the heat transfer coefficient in longitudinal and transverse direction as compared to smooth flat plate and enhancement in both directions, due to the protrusion of the ribs has the effect of promoting turbulence in the wall jet and generates vortexes behind the ribs
2. The stagnation point Nusslet number for both rectangular ribbed surface and circular ribbed surfaces increases with increasing orifice diameter The increase in Nusslet number for ribbed surfaces is the highest for Z/D of 8 as compared to all other orifice plate spacing ratio attributed to maximum centerline turbulent Intensity at this Z/D**.**
3. the enhancement ratio factor (*EF*)in the average heat transfer coefficient when using the rectangular ribbed surface at Z/D=8 for each orifice diameter D=(5,12,20)mm, was approximately (2 to 3) for rectangular ribbed surface with (p/e=5,p/w=1.67), (1.5 to 2) for rectangular ribbed surface with (p/e=3.75,p/w=2.5)and (1.2 to 1.75) for rectangular ribbed surface with(p/e=3.75,p/w=2.5). And the enhancement ratio factor (*EF*)in the average heat transfer coefficient when using the circular ribbed surface was

approximately (2 to 2.5) for circular ribbed surface with (p/e=5) and (1.5 to 2) for circular ribbed surface with (p/e=2.5). This enhancement ratio strongly dependent on the rib geometry and increases with Reynolds number.

Abbreviations

As	Cross sectional area of plate (m^2).
A_{rib}	Total surface area of the two ribs faces (m^2)
D	Orifice diameter (mm)
e	Height of the rib (m^2)
h	Heat transfer coefficient ($W/m^2.C°$)
I	Electrical Current (A)
N	Number of ribs
k_{air}	Thermal conductivity of air at film temperature (W/m.Cº)
k	Thermal conductivity of steel plate (W/m.C°)
L	Length of the rib (m)
Nu	Nusselt number (dimensionless) $= \frac{hD}{K}$
P	Rib pitch
Q_{input}	Total input power (W)
$Q_{rad.}$	Heat losses due to radiation (W)
$Q_{cond.}$	Heat losses due to conduction (W)
$Q_{conv.}$	Heat transfer by convection (W)
$q"_{conv.}$	Heat flux by convection (W/m^2)
R	Orifice radius (mm)
r	Radial distance from the plate center (m)
Re	Reynolds number (dimensionless) $= \frac{U_j D}{\upsilon_j}$
T_f	Film temperature (Cº) $= \frac{T_s + T_j}{2}$
T_s	The temperature at the surface of the plate (Cº)
T_j	The jet-stream temperature (Cº)
U_j	Velocity of air (m/s)
V	Voltage (v).
ν_j	Viscosity of air at film temperature (m^2/s)
ρj	Density of air at film temperature (kg/m^3)
Y	Distance from the plate (mm)
Z	Nozzle-to-plate distance (m)

Acknowledgement

The authors would like to thank the Department of Mechanical Engineering, Al-Mustansiriaya University, for allowing us to use their facilities during this experiment.

6. References

1. Hofmann, Matthias Kind, Holger Martin, 2007, “Measurements on Steady State Heat Transfer and Flow Structure and New Correlations for Heat and Mass Transfer in Submerged Impinging Jets”, International Journal of Heat and Mass Transfer, Vol.50, pp. 3957–3965.
2. VadirajKatti and Prabhu, 2008, “Experimental Study and Theoretical Analysis of Local Heat Transfer Distribution Between Smooth Flat Surface and Impinging Air Jet From a Circular Straight Pipe Nozzle”, International Journal of Heat and Mass Transfer, Vol.51, pp. 4480–4495.
3. Tadhg, Darina and Murray, 2007, “Jet Impingement Heat Transfer – Part I: Mean and root-mean-square heat transfer and velocity distributions”, International Journal of Heat and Mass Transfer, 50, pp. 3291–3301.
4. Attalla and Salem, 2013, “Effect of Nozzle Geometry on Heat Transfer Characteristics from a Single Circular Air Jet”, Journal of Applied Thermal Engineering, 51, pp. 723–733.
5. Gau and Lee, (2000), "Flow and impingement cooling heat transfer along triangular rib roughened walls", International Journal of Heat and Mass Transfer.
6. Hansen and Webb, 1993," Air Jet Impingement Heat Transfer from Modified Surfaces", Int. Jr. Heat Mass Transfer, Vol.36, No.4, PP.989-997.
7. Nakod P.M , S.V. Prabho and R.P Vedola,2006, "Heat transfer augmentation between impinging circular air jet and flat plate using finned surfaces", Heat and Mass Transfer Conference, Indian Institute of Technology (I.I.T.), Guwahati, Paper No:G184,India
8. VadirajKatti and Prabhu , 2013,“Heat transfer enhancement on a flat surface with axisymmetric detached ribs by normal impingement of circular air jet”, Department of Mechanical Engineering, Indian Institute of Technology (I.I.T.), Bombay, Powai, Mumbai 400 076, India
9. Vachirakornwattana, M.Sc. thesis 2012, “Flow structure and heat transfer of air Impingement on a target plate with a single jet”, M.Sc. thesis Teesside University, School of Science and Engineering.